

Accretion Disk Formation Following Tidal Disruption Events Around Spinning Supermassive Black Holes

Kimi Hayasaki (Chungbuk National University, Korea)

In collaboration with Nicholas Stone¹ and Abraham Loeb²

¹Columbia University, USA

²Harvard-Smithsonian Center for Astrophysics, USA

17/Mar/2016@KASI



Outline

1. Introduction

- a. Tidal disruption events (TDEs)
- b. Standard picture of TDEs
- c. Concept of “eccentric” TDEs
- d. Our goal

2. Difference between parabolic and eccentric TDEs

Numerical modeling of a star-black hole system by SPH

3. Disk formation around non-spinning SMBH in eccentric TDEs

General relativistic (GR) treatment in SPH (Pseudo-Newtonian Approach)

4. Effect of SMBH spin on debris circularization

GR treatment in SPH (Post-Newtonian Approach)

5. Summary

1. Introduction

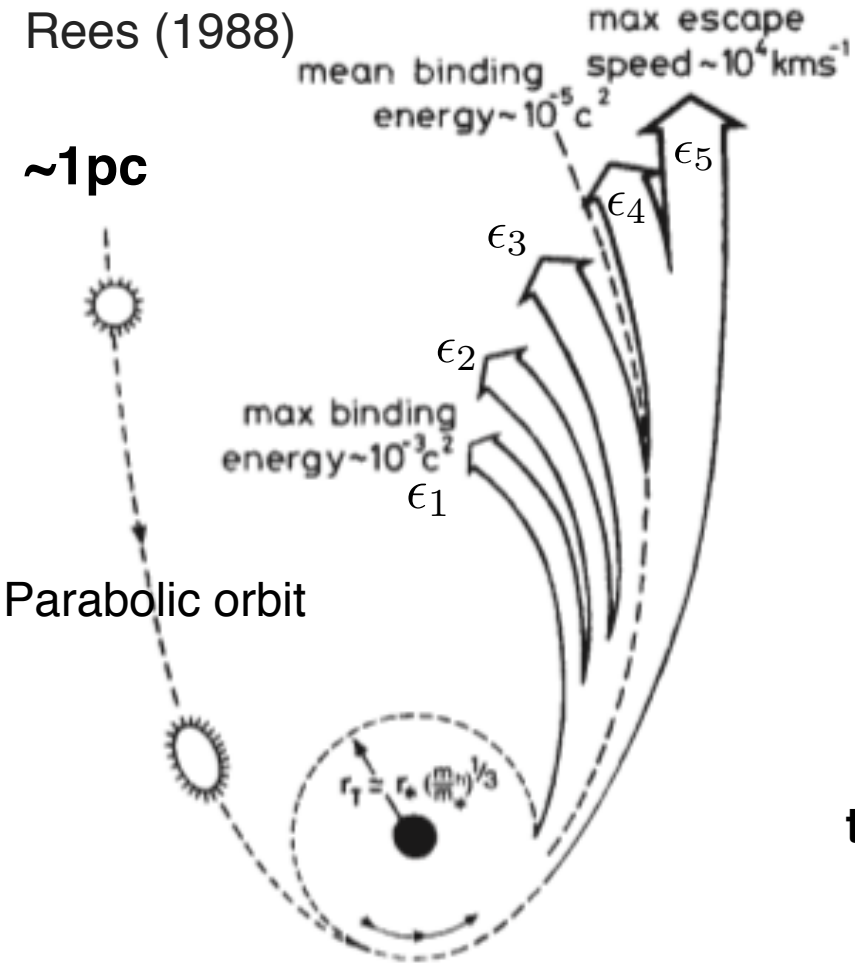
Scientific motivations for TDEs

1. Probe of quiescent supermassive black holes (SMBHs)
2. Laboratory for super-Eddington accretion and outflow physics
3. One of gravitational wave source candidates

Good phenomena for multi-messenger astronomy

Tidal Disruption of a star by a SMBH

Standard Picture



Tidal disruption radius
(Tidal force=self-gravity force):

$$r_t = \left(\frac{M_{BH}}{m_*} \right)^{1/3} r_*$$

$\Delta\epsilon$: Spread in debris energy by tidal force

$$\Delta\epsilon = \frac{GM_{BH}}{r_t} \frac{r_*}{r_t}$$

ϵ : Debris specific energy

- if $\epsilon \geq 0$ Stellar debris flies away from the black hole
- if $\epsilon < 0$ Stellar debris is bounded by the black hole's gravity and falls back to black hole

t : Fallback time for most tightly bound debris

$$t_{fall} \sim 0.1 \text{ yr} \left(\frac{r_*}{R_\odot} \right)^{3/2} \left(\frac{m_*}{M_\odot} \right)^{-1} \left(\frac{M_{BH}}{10^6 M_\odot} \right)^{1/2}$$

What is the rate of mass fallback?

Mass fallback rate I.

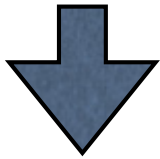
$$\frac{dM}{dt} = \frac{dM(\epsilon)}{d\epsilon} \left| \frac{d\epsilon}{dt} \right| \quad (\epsilon < 0)$$

Specific energy: $\epsilon \approx -\frac{GM_{\text{BH}}}{2a}$

Its time derivative:

$$\frac{d\epsilon}{dt} = -\frac{1}{3} (2\pi GM_{\text{BH}})^{2/3} t^{-5/3}$$

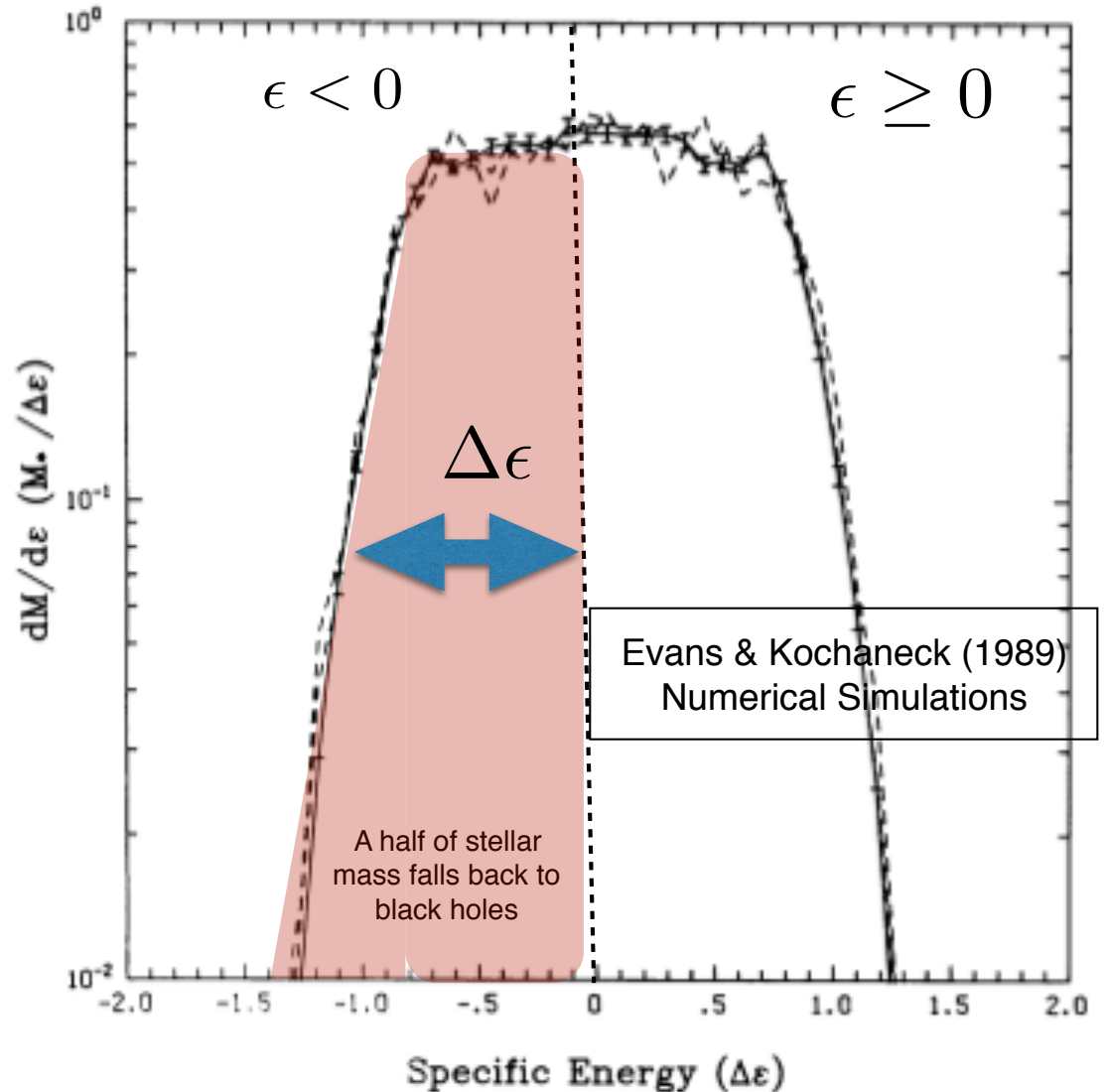
(by using Keplerian third law)



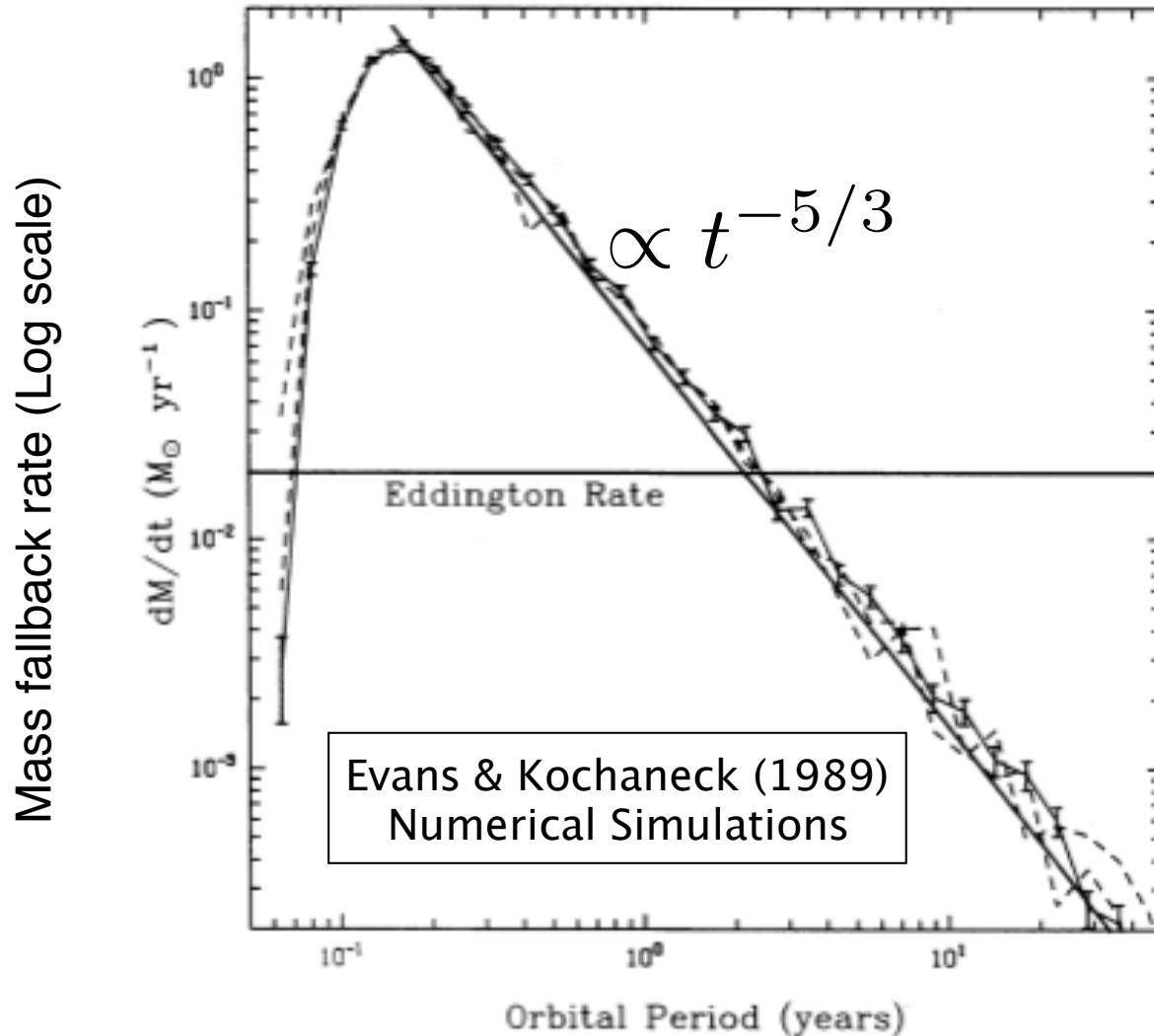
$$\frac{dM}{dt} \propto t^{-5/3}$$

Rees's conjecture (1988)

Differential mass-energy distribution of stellar debris



Mass fallback rate II.

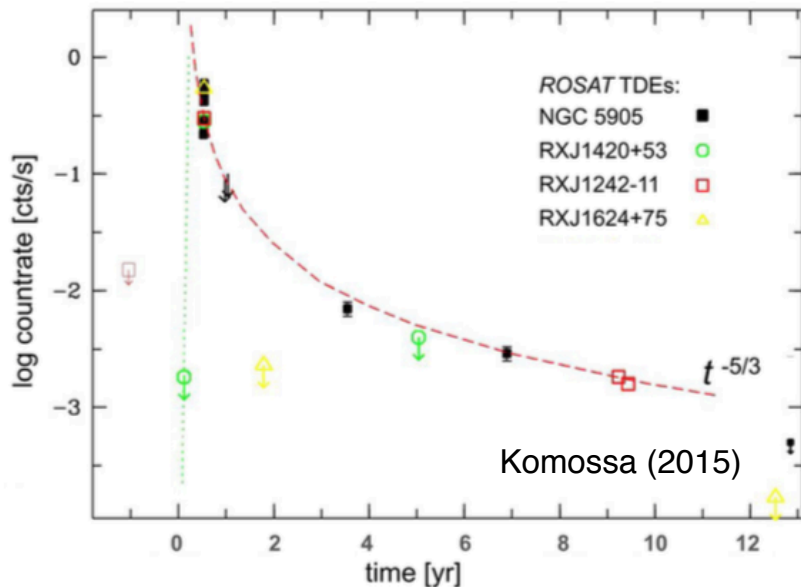


Laguna et al. (1993);
Ayal et al. (2001);
Enrico & Rosswog (2009);
Guillocheon et al. (2011, 2012, 2013,
2014..); Shiohara et al. (2015)

**Rees's conjecture is consistent
with numerical simulations**

Observed TDE candidates

- 33 candidates (~20 are discovered during 2011-15)
- Event rate: $10^{-4} \sim 10^{-5}$ per galaxy [1/year] (Donley + 2002; Wang & Merritt 2004; Stone & Mezer 2015)
- Observed optical to X-ray light curves follow $t^{-5/3}$ law, whereas some do not



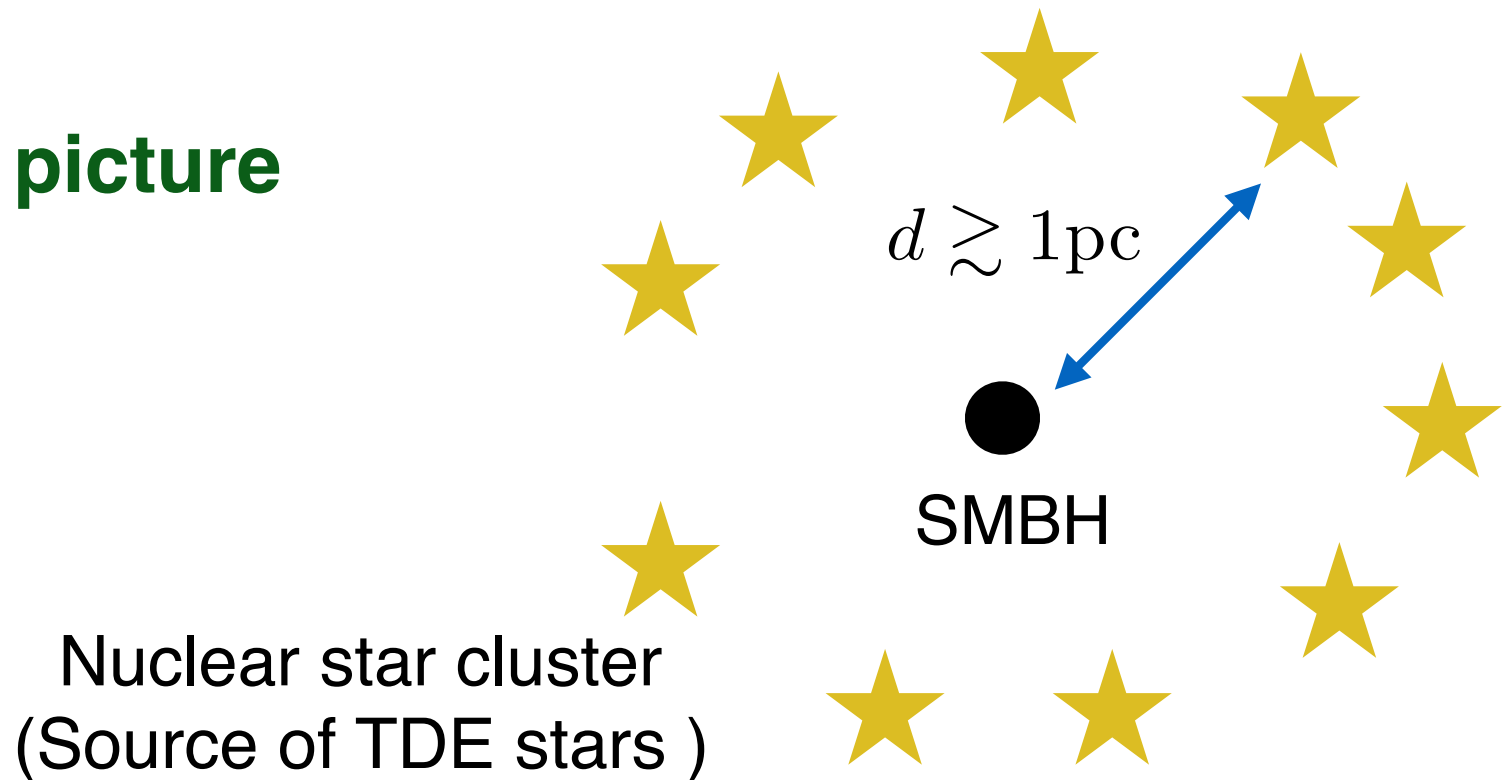
Komossa (2015)

source name	redshift	discovery mission	reference
soft X-ray events			
NGC 5905	0.011	<i>ROSAT</i>	Bade et al. 1996, Komossa & Bade 1999
RX J1242–1119	0.050	<i>ROSAT</i>	Komossa & Greiner 1999
RX J1624+7554	0.064	<i>ROSAT</i>	Grupe et al. 1999
RX J1420+5334	0.147	<i>ROSAT</i>	Greiner et al. 2000
NGC 3599	0.003	<i>XMM-Newton</i>	Esquej et al. 2007, 2008
SDSS J1323+4827	0.087	<i>XMM-Newton</i>	Esquej et al. 2007, 2008
TDXF 1347–3254	0.037	<i>ROSAT</i>	Cappelluti et al. 2009
SDSS J1311–0123	0.195	<i>Chandra</i>	Maksym et al. 2010
2XMMi 1847–6317	0.035	<i>XMM-Newton</i>	Lin et al. 2011
SDSS J1201+3003	0.146	<i>XMM-Newton</i>	Saxton et al. 2012
WINGS J1348	0.062	<i>Chandra</i>	Maksym et al. 2013, Donato et al. 2014
RBS1032	0.026	<i>ROSAT</i>	Maksym et al. 2014b, Khabibullin & Sazonov 2014
3XMM J1521+0749	0.179	<i>XMM-Newton</i>	Lin et al. 2015
hard X-ray events			
Swift J1644+57	0.353	<i>Swift</i>	Bloom et al. 2011, Burrows et al. 2011, Levan et al. 2011, Zauderer et al. 2011
Swift J2058+0516	1.186	<i>Swift</i>	Cenko et al. 2012b
UV events			
J1419+5252	0.370	<i>GALEX</i>	Gezari et al. 2006
J0225–0432	0.326	<i>GALEX</i>	Gezari et al. 2008
J2331+0017	0.186	<i>GALEX</i>	Gezari et al. 2009
optical events			
SDSS J0952+2143 ¹	0.079	SDSS	Komossa et al. 2008
SDSS J0748+4712 ¹	0.062	SDSS	Wang et al. 2011
SDSS J2342+0106	0.136	SDSS	van Velzen et al. 2011
SDSS J2323–0108	0.251	SDSS	
PTF 10iya	0.224	PTF	Cenko et al. 2012a
SDSS J1342+0530 ¹	0.034	SDSS	Wang et al. 2012
SDSS J1350+2916 ¹	0.078	SDSS	
PS1–10jh	0.170	Pan-STARRS	Gezari et al. 2012
ASASSN–14ae	0.044	ASAS-SN	Holoien et al. 2014
PTF 09ge	0.064	PTF	Arcavi et al. 2014
PTF 09axc ²	0.115	PTF	
PTF 09djl	0.184	PTF	
PTF 10nuj ³	0.132	PTF	
PTF 11glr ³	0.207	PTF	
PS1–11af	0.405	Pan-STARRS	Chornock et al. 2014

Question

Stars fall to SMBH only on parabolic orbits?

Standard picture



Binding energy: $\epsilon = -\frac{GM_{\text{bh}}}{2d} \sim 0 \rightarrow$ Parabolic orbit!

Possibility for approaching stars on eccentric orbits

Historically, TDE theory considers parabolic orbits: Well-motivated for 2-body scattering (bulge), large-scale triaxiality (galaxy)

More exotic contributions to TDE rate have been proposed recently:

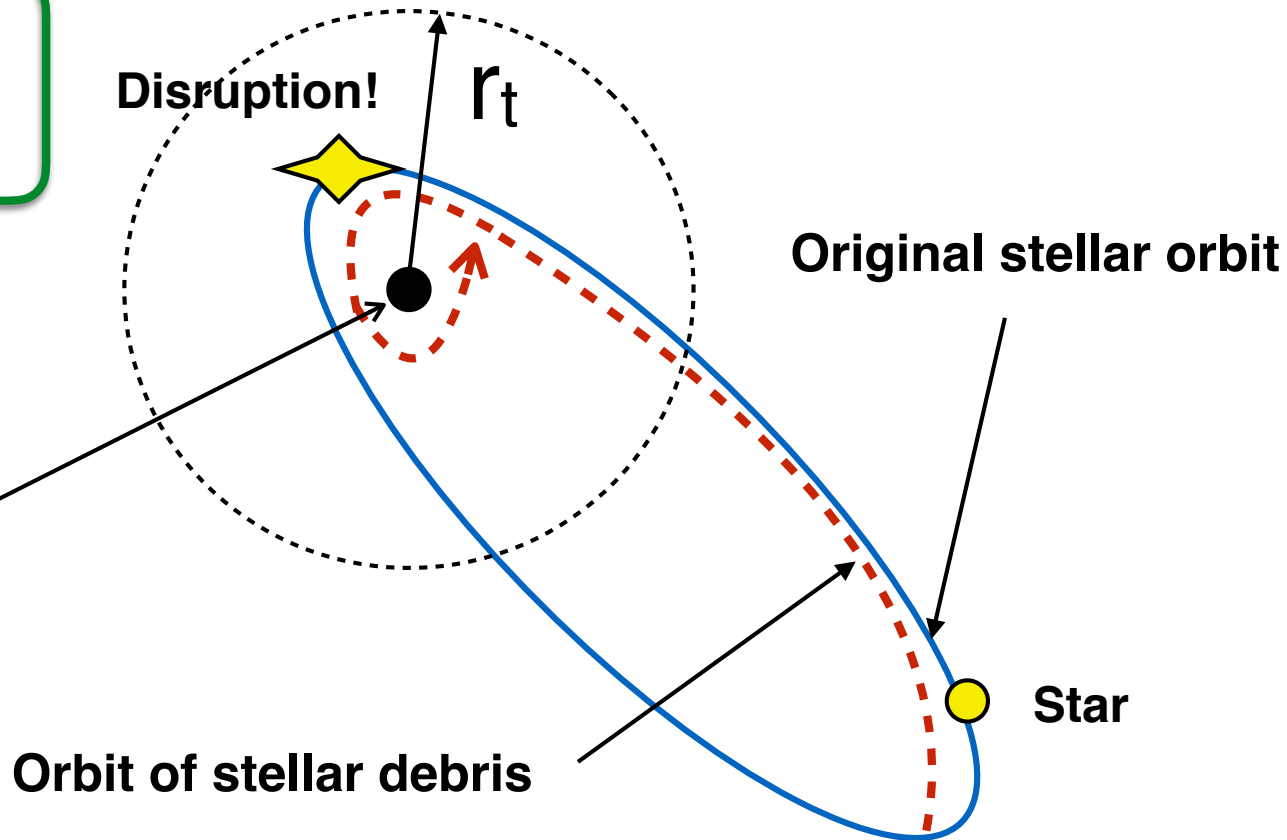
- Binary star separation (Amaro-Seoane+2012, Bromley+ 2012)
- Recoiling SMBH (Stone & Loeb 2011)
- Kozai-Lidov mechanism in SMBH binaries (Chen+2009,2011; Seto & Muto 2010,2011; Li et al.2015)

These mechanism makes smaller eccentricities possible than $e=1$ ($0.1 < e < 1$)

Our Goal

A schematic picture of “**Eccentric TDEs**”

**Non-spinning /
spinning SMBH**



1. To find differences between parabolic and eccentric (or bound) TDEs

2. To study effect of SMBH spin on debris circularization in eccentric TDEs

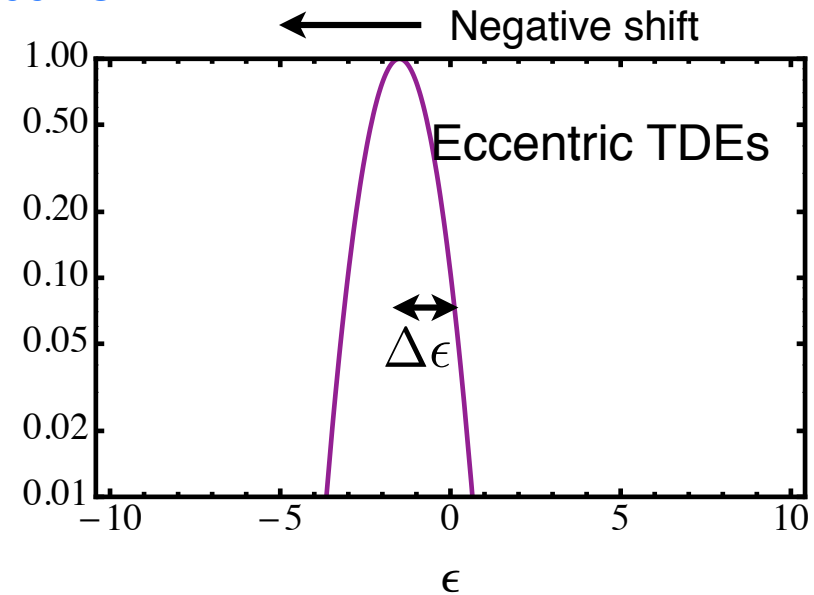
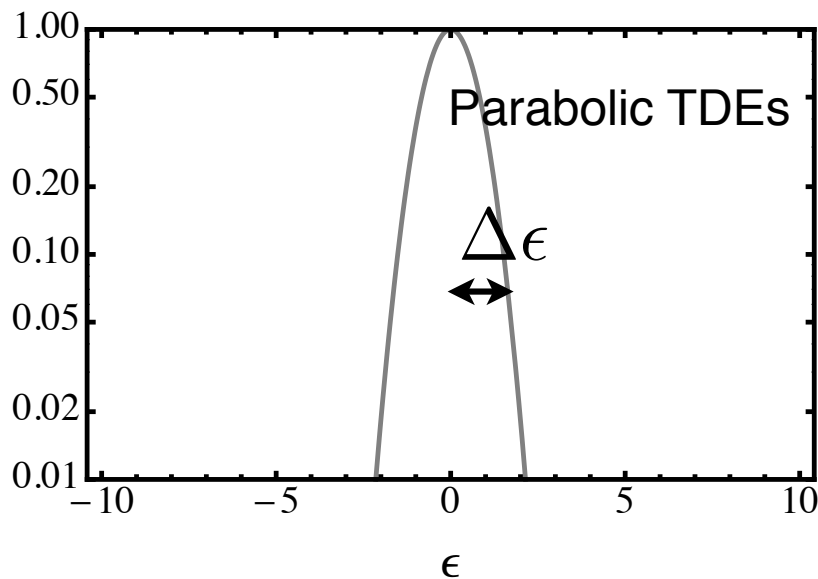
2. Differences between parabolic and eccentric TDEs

Theoretical expectation in “Eccentric” TDEs

Hayasaki, Stone & Loeb (2013)

All of stellar debris are bounded by black hole even after the tidal disruption, if $\Delta\epsilon \leq |\epsilon_{\text{orb}}|$

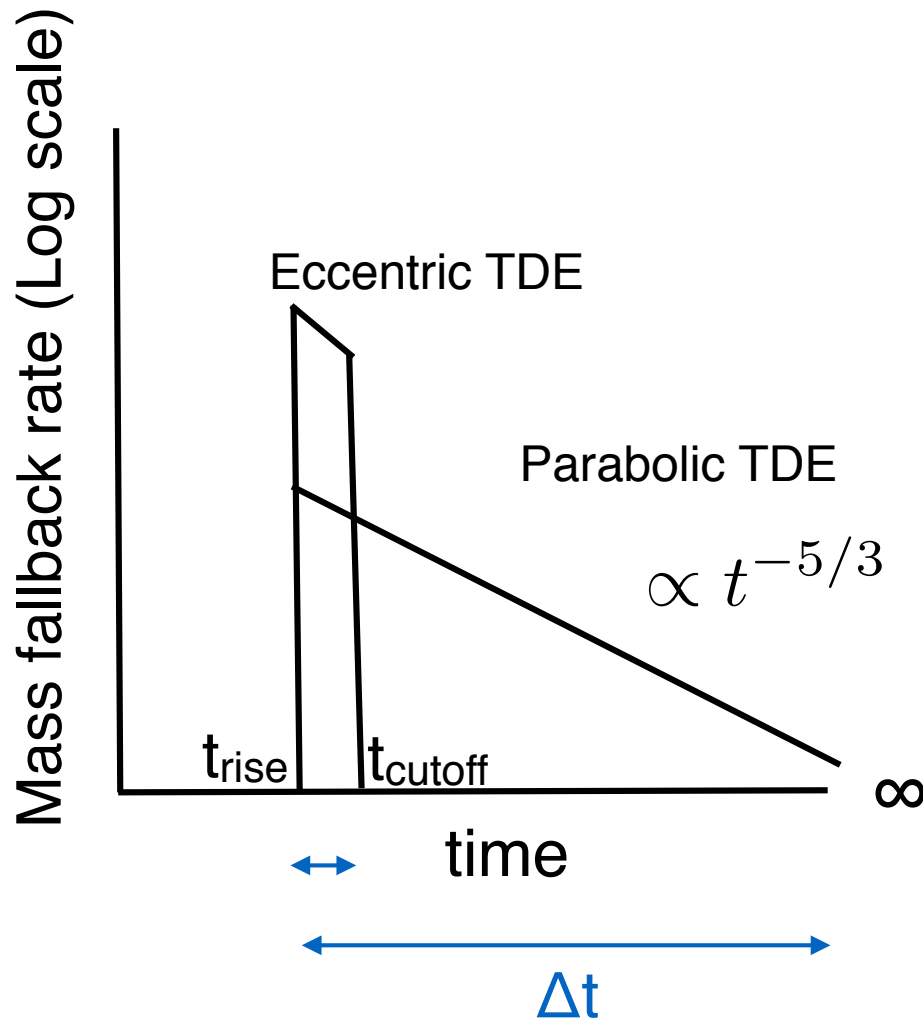
Mass distribution



All of disrupted mass can fall back to black hole if $e < e_{\text{crit}}$.

$$\left. \begin{aligned} \Delta\epsilon &= \frac{GM_{\text{BH}}}{r_t^2} r_* \\ \epsilon_{\text{orb}} &\approx -\frac{GM_{\text{BH}}}{2r_t} \beta (1 - e_*) \end{aligned} \right\} \longrightarrow e_{\text{crit}} \approx 1 - \frac{2}{\beta} \left(\frac{M_{\text{BH}}}{m_*} \right)^{-1/3}, \quad \beta = \frac{r_t}{r_p}$$

Difference of \dot{M} between two type of TDEs



\dot{M} is much higher than that of parabolic TDE

1. All of stellar mass fall back to SMBH
2. Much shorter duration time: Δt

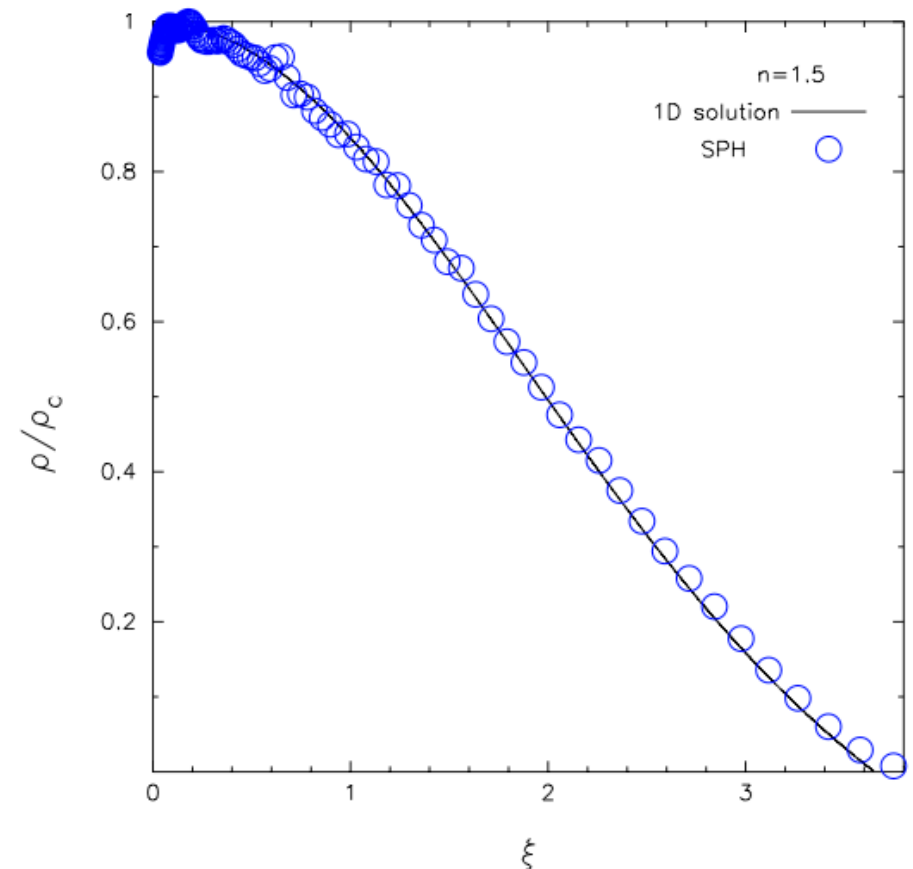
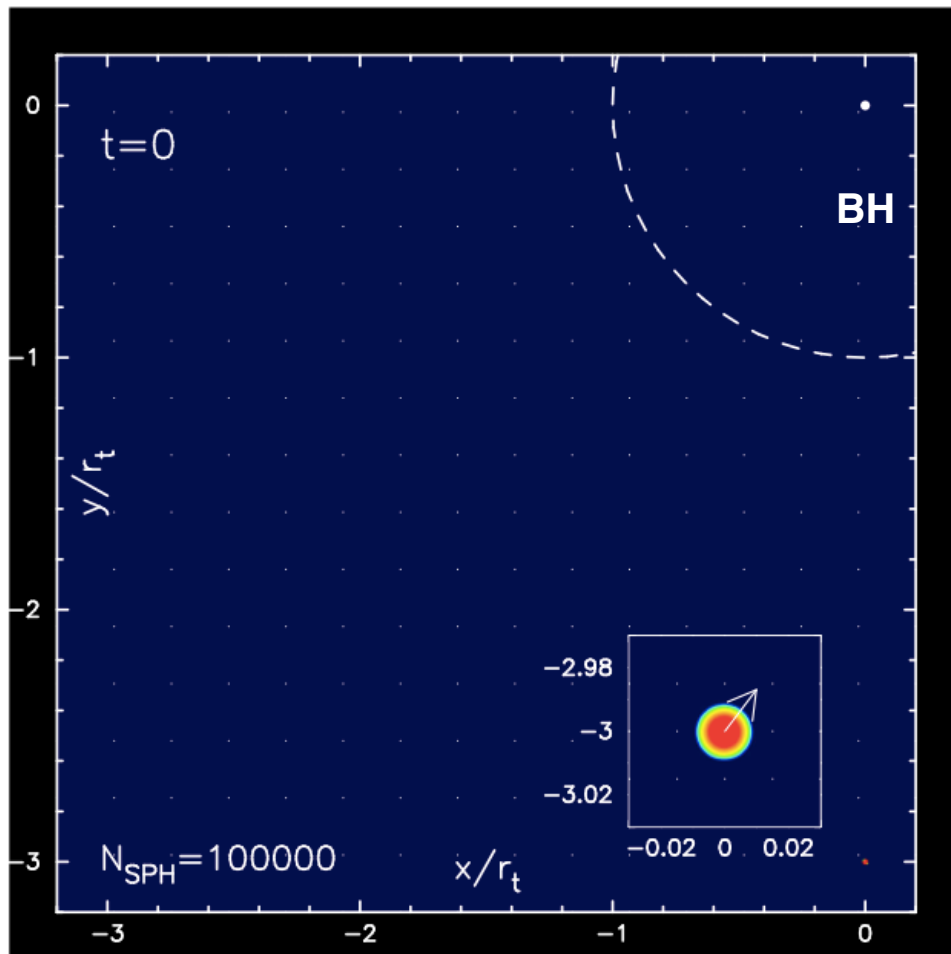
$$\dot{M}_{\text{fall}} \sim m_* / \Delta t$$

We tested them by numerical simulations (Hayasaki et al. 2013)

Modeling of star-black hole system

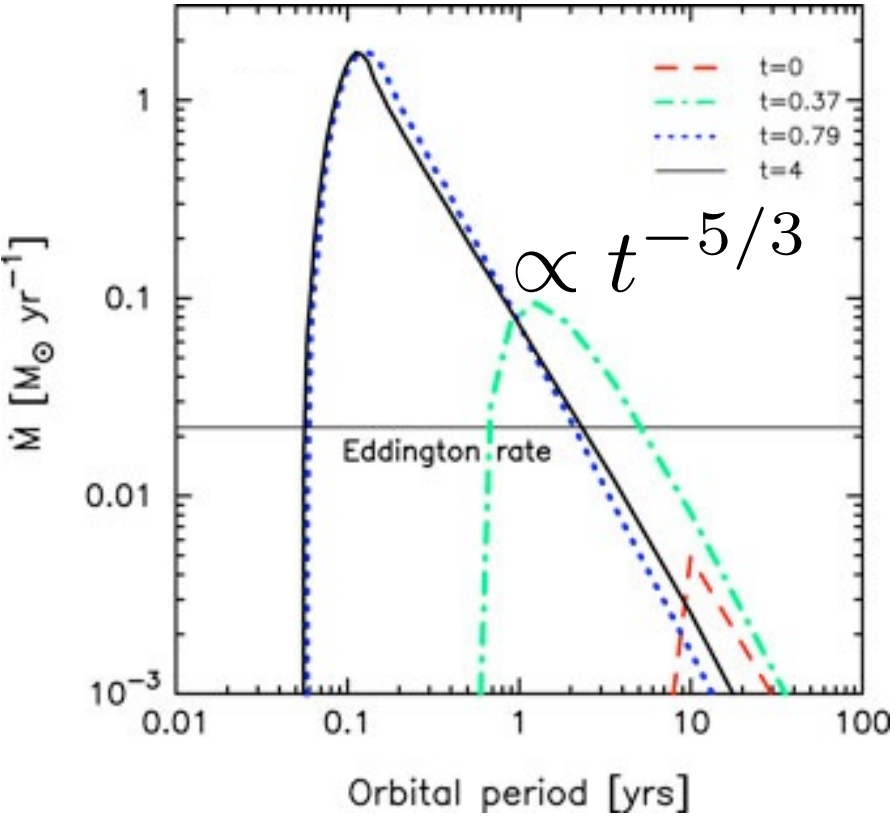
SPH code: Benz(1990); Bate et al.(1995)

BH mass : $M_{\text{bh}} = 10^6 M_{\odot}$ **Stellar mass :** $M_{\text{star}} = 1 M_{\odot}$ **Eq. of state :** polytrope
Stellar radius : $R_{\text{star}} = 1 R_{\odot}$ **(index : n = 1.5)**

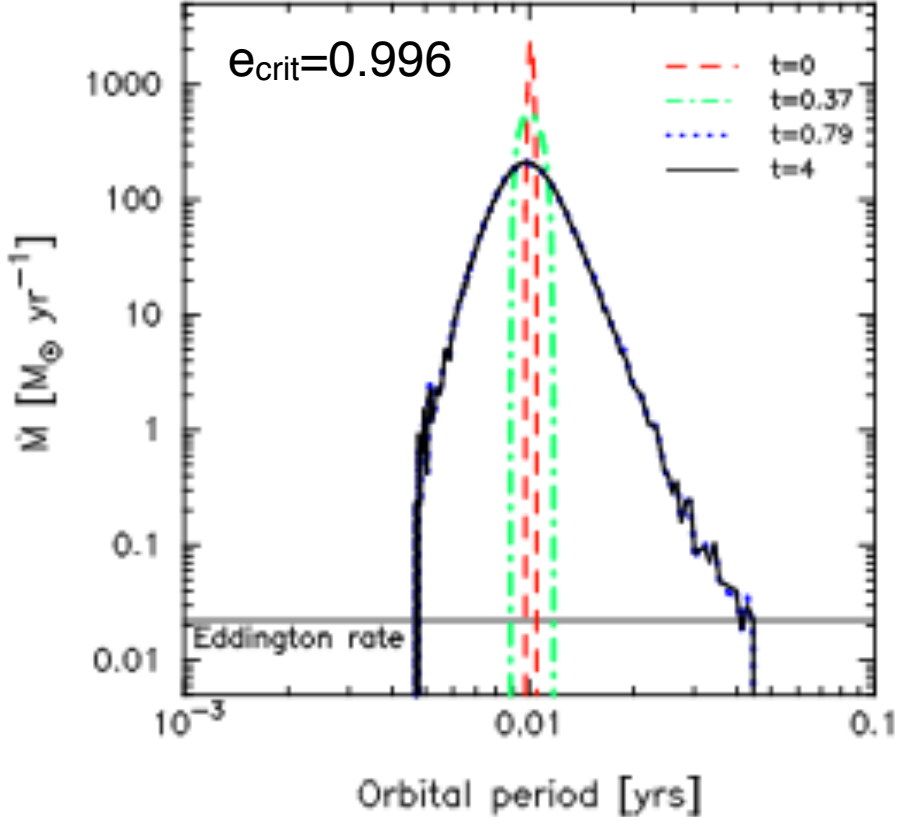


Comparison between parabolic and eccentric TDEs

Parabolic (Standard) TDE



Eccentric TDE $e=0.98$ and $\beta=5$



Mass fallback rate has clearly a finite cut-off time and is ~ 200 times larger than that of standard TDEs

**Light curve is different between
parabolic ($\epsilon=0$) and eccentric ($\epsilon<0$)
TDEs, if it is proportional to mass
fallback rate**

Differences between Parabolic and Eccentric TDEs

	Original stellar orbit	Peak value of mass fallback rate [\dot{M}_{Edd}]	Mass-fallback-rate curve	The Number of observed TDE candidates	Typical fallback timescale [$2\pi\sqrt{r_t^3/GM}$]
Parabolic, standard TDEs	Parabolic ($\varepsilon=0$)	$\sim 10^{2-3}$	$t^{-5/3}$	~ 30 Komossa&Bode 1999; Maksym et al.2010; Burrows et al. 2011; Arcavi et al. Gezari et al. (2009,2012); 2014; Holoien et al 2014; Vinko et al.2015, and more	~ 350
Eccentric TDEs	Eccentric ($\varepsilon<0$)	$\sim 10^{4-6}$	Steeper	1 [Campana et al.(2015)]	~ 10

Easier to simulate fallback process in eccentric TDEs because of much shorter simulation run time

3. Disk Formation around non-spinning SMBH in eccentric TDEs

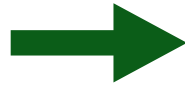
Hayasaki, Stone & Loeb (2013)

Motivation

1st Question

1. Stellar debris falls back to not directly SMBH but periastron
2. Accretion disk should be formed in order to cause TD flare
3. Orbital energy of debris should be lost by any mechanism

How ?



Shock energy dissipation
of stellar debris

(Rees 1988, Cannizzo et al. 1990, Kochanek 1994; Kim et al. 1999)

2nd Question

What is mechanism to cause it ?

1. Tidal compression at periastron

(Carter & Luminet 1982; Ramirez-Ruiz & Rosswog 2009; Guillochon et al. 2013)

2. Debris self-crossings by GR perihelion shift

(Rees 1988; Hayasaki et al. (2013,2015); Shiokawa et al. 2015; Bonnerot 2016)

How to treat GR effect (Schwarzschild space-time)

For simple GR treatment, pseudo Newtonian potential is incorporated into the SPH code.

Wegg (2012):

$$U(r) = c_1 \frac{GM_{\text{BH}}}{r} - \frac{(1 - c_1)GM_{\text{BH}}}{r - c_2 r_g} - \frac{c_3 GM_{\text{BH}}}{r} \frac{r_g}{r}$$

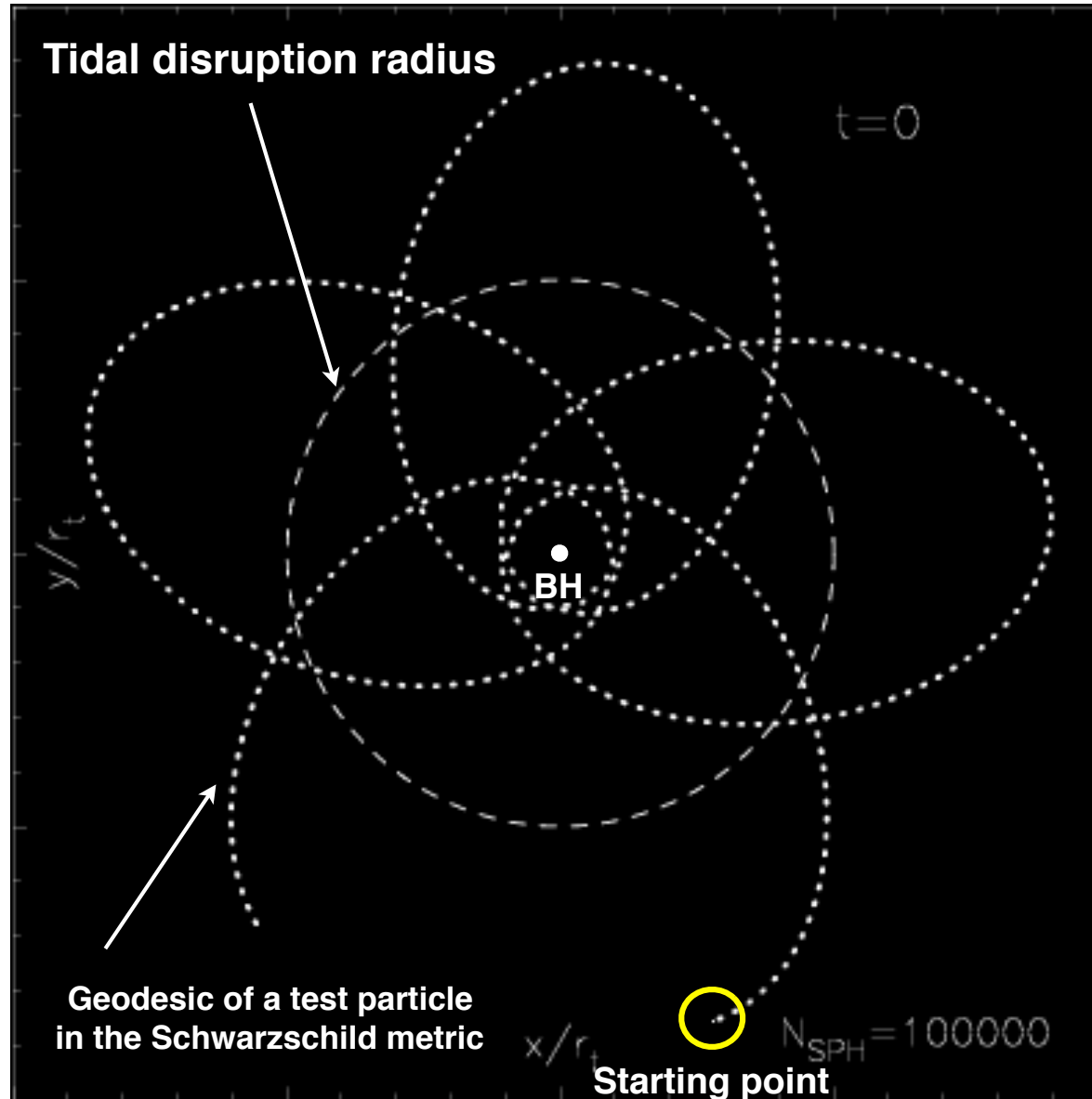
where $c_1 = -(4/3)(2+6^{1/2})$, $c_2 = 4*6^{1/2}-9$, $c_3 = -(4/3)(2*6^{1/2}-3)$

Newtonian if
 $c_1=1, c_2=c_3=0$

Paczynski-Wiita PN
if $c_1=c_3=0, c_2=1$

We modeled only GR apsidal precession by incorporating pseudo-Newtonian potential (Wegg 2012) into SPH code

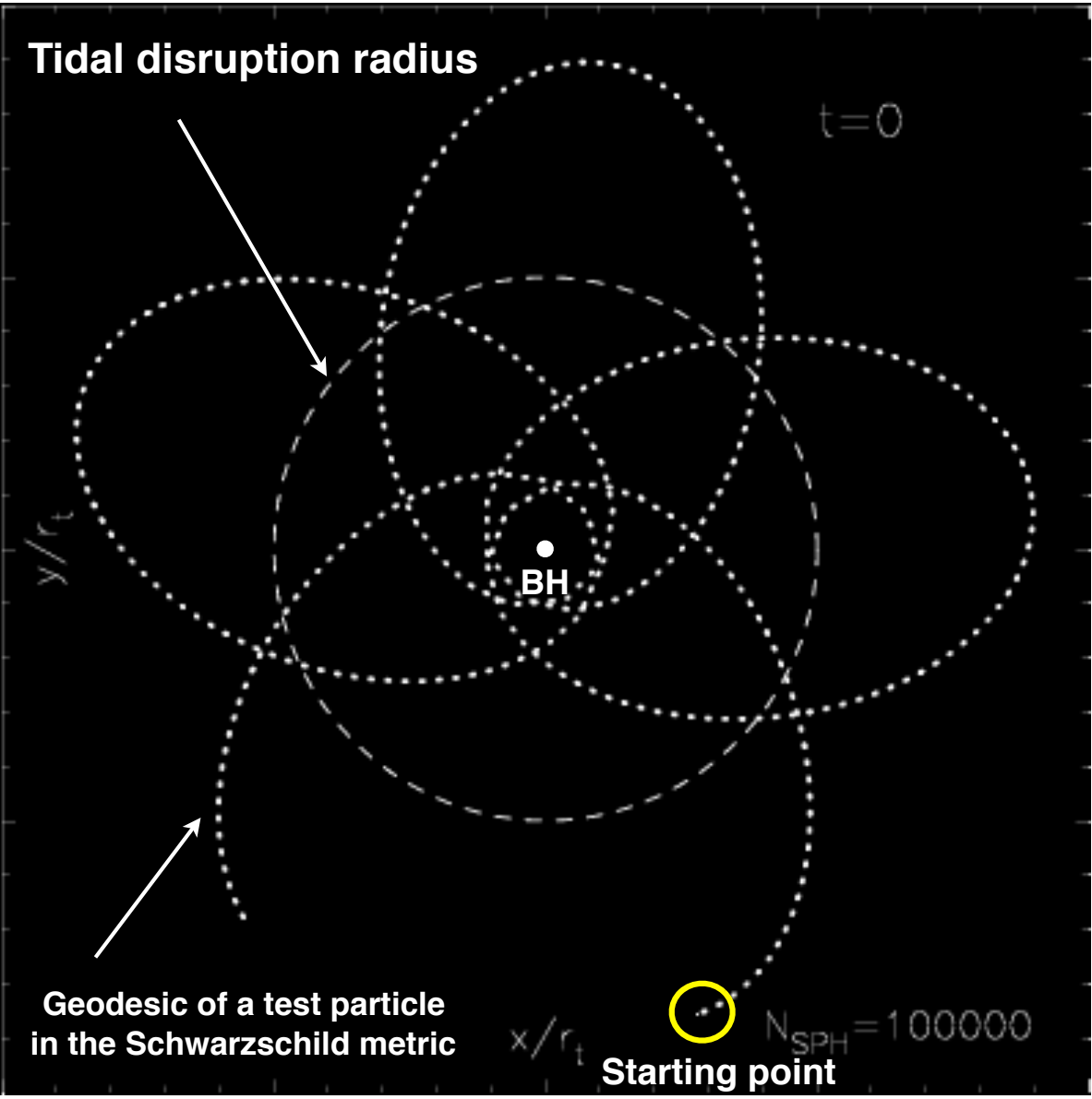
Newtonian potential simulation



- Dotted line shows the geodesic of a test particle
- Dashed circle shows the tidal disruption radius
- Central point represents the black hole

**Stellar debris orbits around SMBH,
following Keplerian third law**

Simulation with GR corrections by Pseudo-Newtonian



- Dotted line shows the geodesic of a test particle
- Dashed circle shows the tidal disruption radius
- Central point represents the black hole

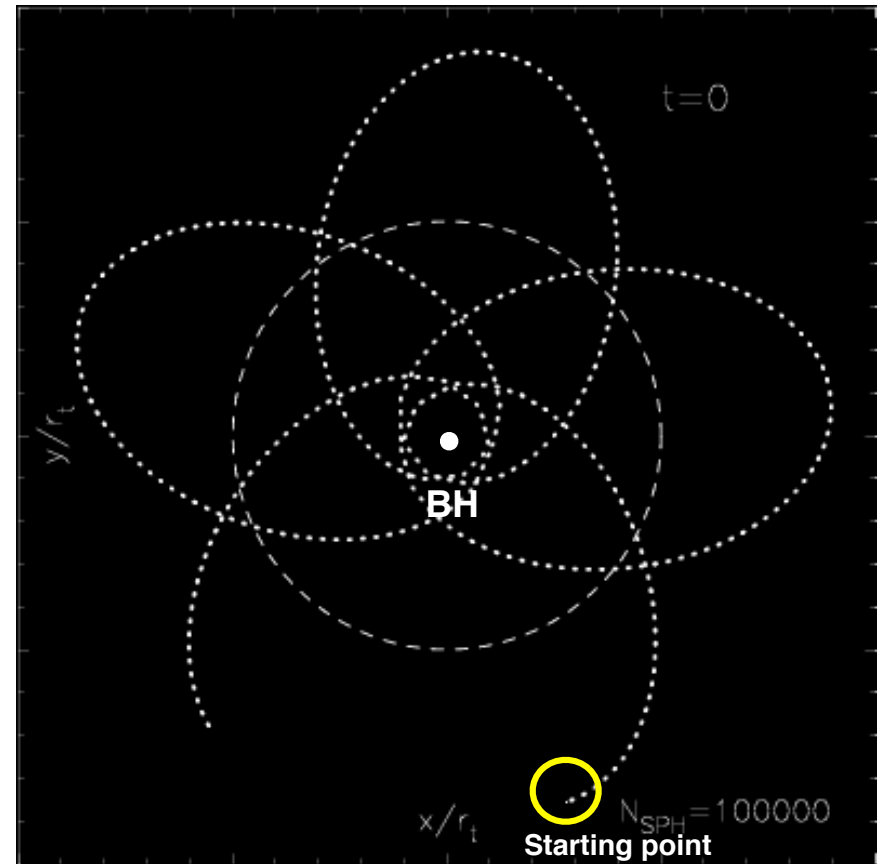
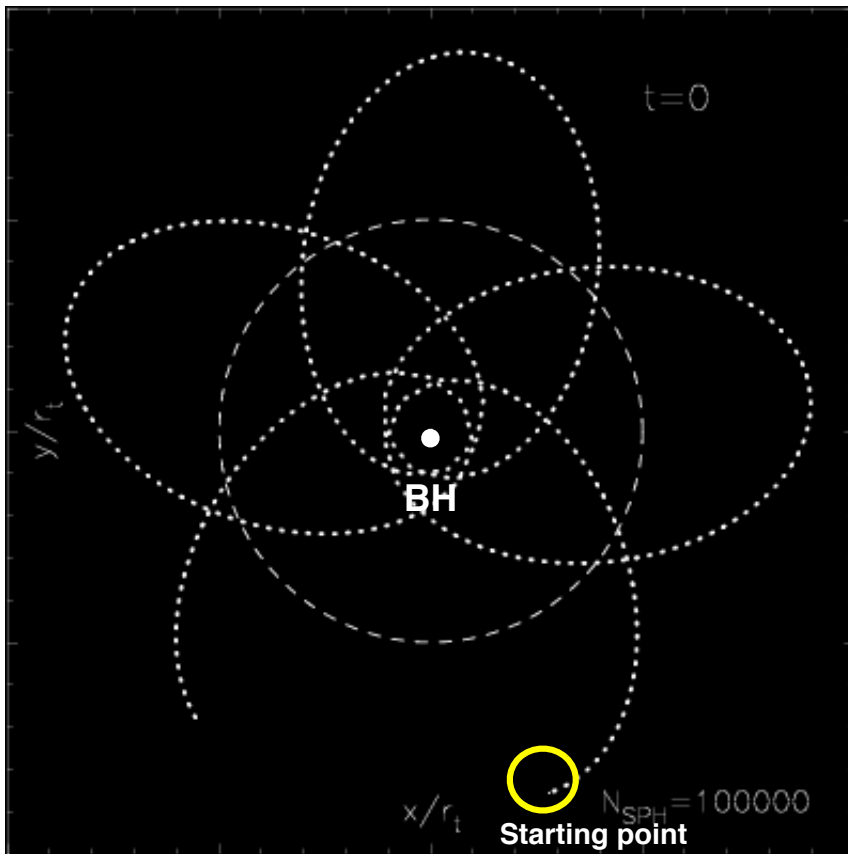
Accretion disk is formed around the black hole due to shock energy dissipation of orbital crossings induced by perihelion shift

Comparison of two animations

Hayasaki, Stone & Loeb (2013)

Newtonian potential simulation

Simulation with GR corrections



General relativistic precession plays a crucial role in the accretion disk formation around supermassive black hole

4. Effect of SMBH spin on Debris Circularization

Hayasaki, Stone & Loeb., arXiv:1501.05207

For Kerr black hole case, pseudo-Newtonian potential is not available any more

Treatment of GR effects including BH spin

1. General Relativity

Einstein equation

$$G_{\mu\nu} = \frac{8\pi G}{c^4} T_{\mu\nu}$$

Geodesic equation

$$\frac{d^2 x^\lambda}{d\tau^2} + \Gamma_{\mu\nu}^\lambda \frac{dx^\mu}{d\tau} \frac{dx^\nu}{d\tau} = 0$$

Post-Newtonian (PN) Approach

1. Metric can be expressed by deviations from Minkowski spacetime ($v \ll c$)
2. Substituting expanded metric into the geodesic equation

2. Test particle's eq. of motion with PN corrections

PN corrections

$$\frac{d\vec{v}}{dt} = \underbrace{\left(\frac{v'}{c}\right)^0 \vec{a}_{0\text{PN}}}_{\text{Newtonian acceleration}} + \underbrace{\left(\frac{v'}{c}\right)^2 \vec{a}_{1\text{PN}}}_{\text{1 PN acceleration}} + \underbrace{\left(\frac{v'}{c}\right)^3 \vec{a}_{1.5\text{PN}}}_{\text{Spin-induced (1.5PN) acceleration}} + \underbrace{\left(\frac{v'}{c}\right)^4 \vec{a}_{2\text{PN}}}_{\text{2 PN acceleration}}$$

Blanchet (2006)

PN accelerations are incorporated into SPH equation of motion

Simple PN treatment in SPH

Order of magnitude estimate of each term in fluid equation of motion

Hayasaki, Stone & Loeb, (arXiv:1501.05207)

$$\mathcal{O}(v^2/c^2) = 10^{-2} \quad \text{1PN gravitational acceleration}$$

$$\mathcal{O}(c_s^2/c^2) = 10^{-5} \quad \text{1PN Pressure term}$$

$$\mathcal{O}(v_{\text{sg}}^2/c^2) = \mathcal{O}(v^2/c^2 [m_*/M_{\text{BH}}]^{2/3}) = 10^{-6}$$

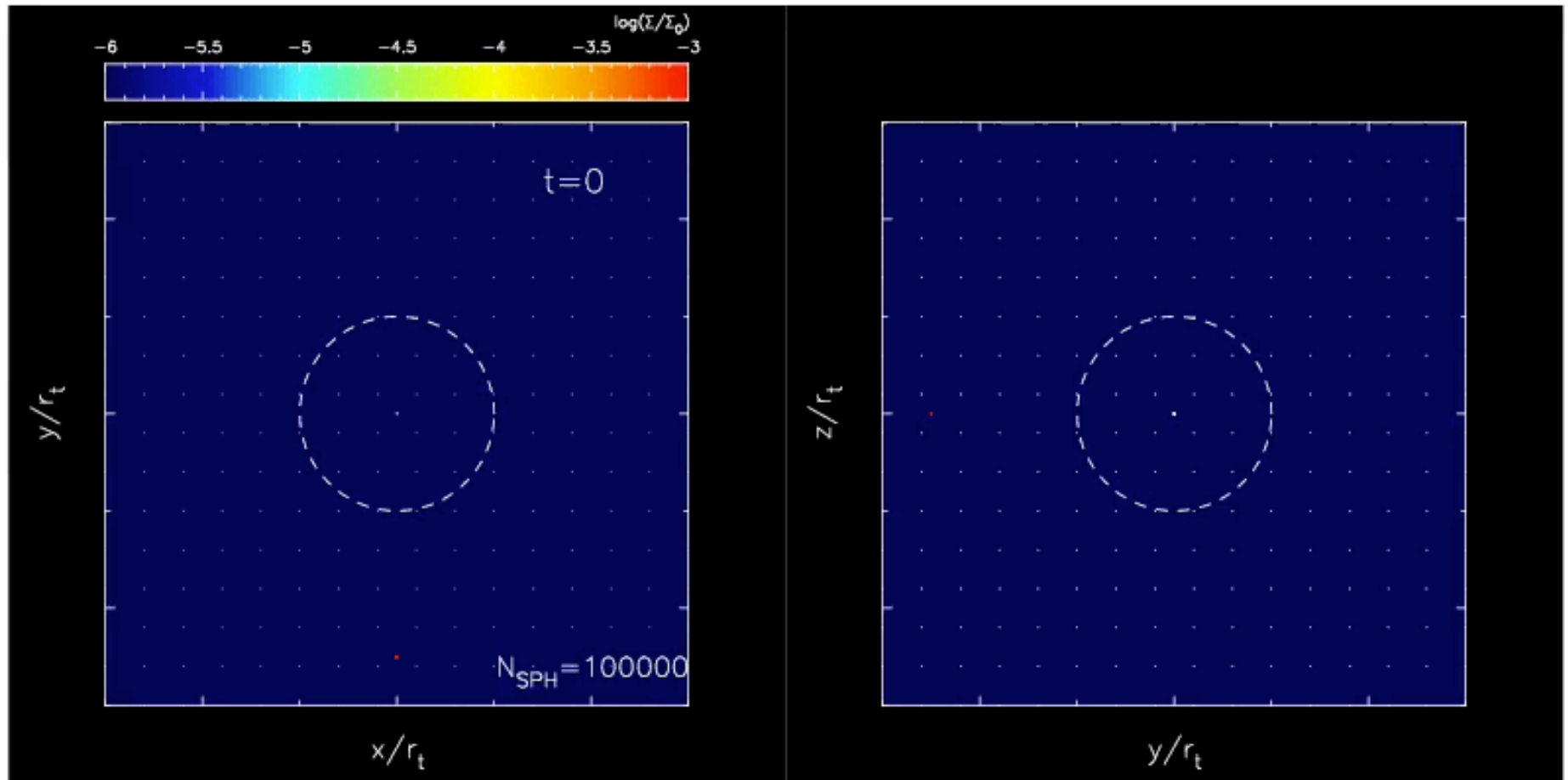
1PN self-gravitation term

Hydro-dynamic and self-gravitating terms can be neglected in fluid equation of motion up to 2PN gravitational acceleration term [see Binachet et al.(1990) for full PN treatment; Ayal et al. (2001a,b) for full but 1+2.5PN. see also Laguna (1993a,b) and Rosswog (2009) for Schwarzschild metric]

Effect of SMBH spin on debris circularization

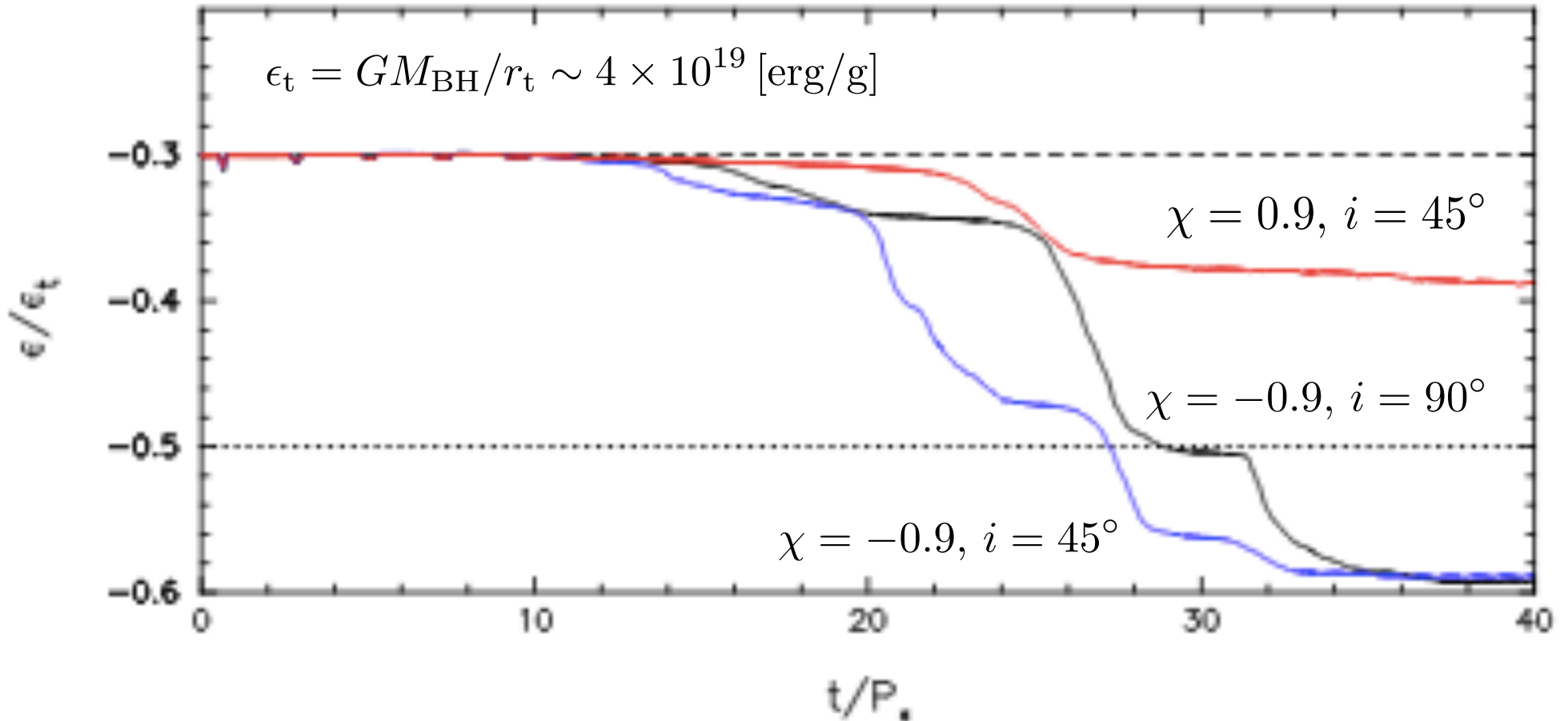
Hayasaki, Stone, & Loeb (2015)

$$a_* = 5/3, e_* = 0.7, \beta = 2, \chi = -0.9, i = 90^\circ$$



Disk precesses around BH spin axis by Lense-Thirring Torque

Evolution of debris specific energy



1. Energy evolution curve is sensitive to black hole spin
2. Positive spin case significantly delays debris circularization

Summary & Discussion

- Eccentric TDEs have critical value of eccentricity, below which all mass is bounded by black hole. Since fallback time is finite when $e < e_{\text{crit}}$, mass fallback rate substantially exceeds Eddington rate.
- GR (perihelion shift) plays an important role in accretion disk formation via circularization of stellar debris from stars on moderately eccentric orbits.
- Post-Newtonian approach is an effective tool to study SMBH spin effect on debris circularization
- Lense-Thirring effect is observable if radiative cooling is efficient. We will have to examine it more by using RHD code

**Thank you for
your attention**

Radiative cooling efficiency II.

$t_{\text{fb}} > t_{\text{diff}}$ Debris orbital energy is converted to thermal energy by shock and radiated away

$t_{\text{fb}} < t_{\text{diff}}$ Debris orbital energy is converted to thermal energy by shock and stored into debris

It is not so simple to treat radiative transfer in optically thick region

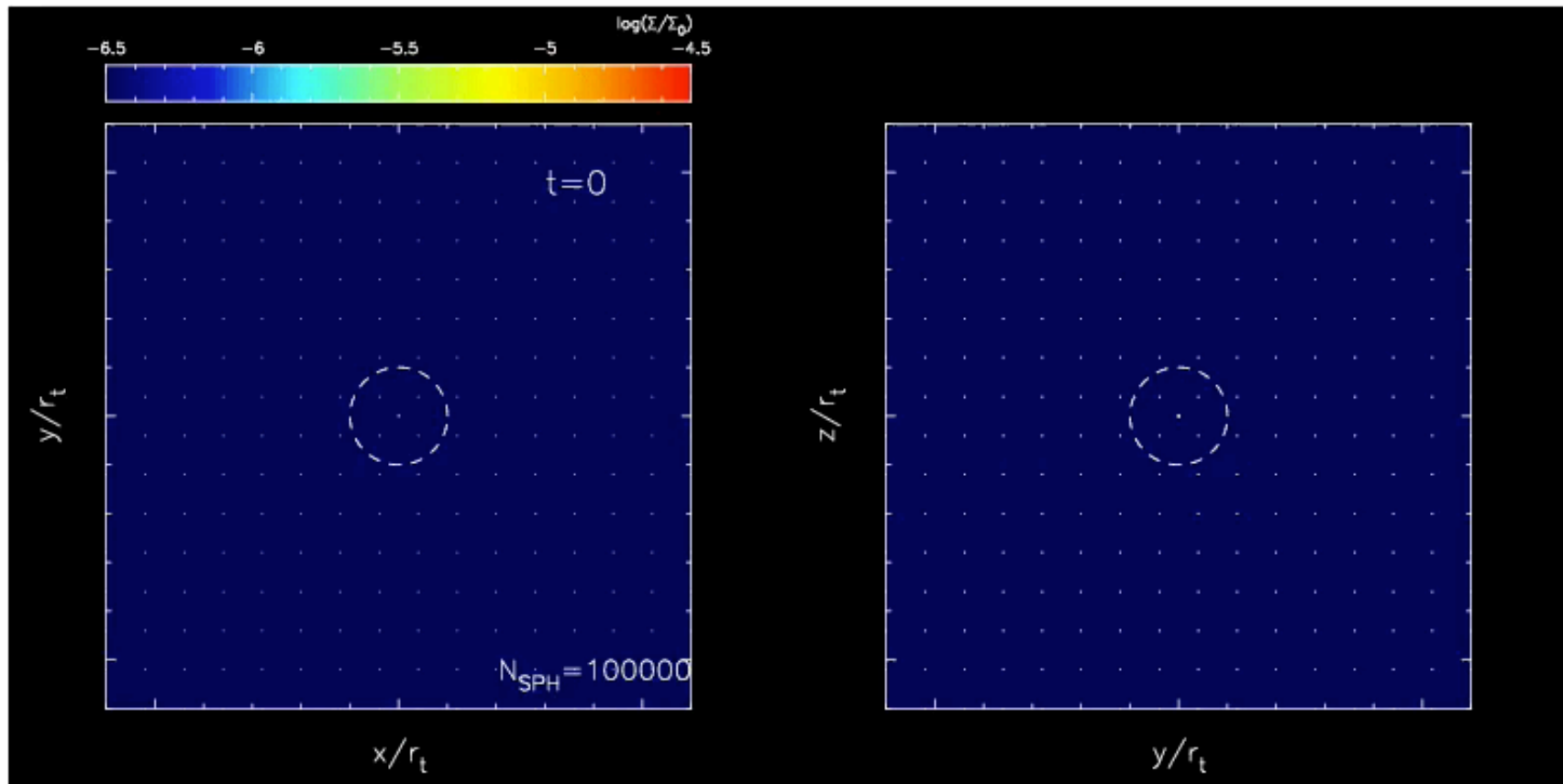
$t_{\text{fb}} \gg t_{\text{diff}}$ **Radiatively efficient cooling case**
(iso-entropy following polytropic law)

$t_{\text{fb}} \ll t_{\text{diff}}$ **Radiatively inefficient cooling case**
(globally adiabatic but locally entropy change)

We consider two extreme cases

Radiatively inefficient cooling case

$$a_* = 5/3, e_* = 0.7, \beta = 2, \chi = -0.9, i = 90^\circ$$



Lense-Thirring precession timescale is remarkably long (much longer than viscous timescale)